Bioheat transfer in the human eye: a boundary element approach

E. H. Ooi, W. T. Ang* and E. Y. K. Ng
School of Mechanical and Aerospace Engineering
Nanyang Technological University
50 Nanyang Avenue, Singapore 639798

Abstract

A boundary element method is applied for the numerical solution of a boundary value problem for a two-dimensional steady-state bioheat transfer model of the human eye. The human eye is modeled as comprising four distinct homogeneous regions. The boundary condition on the outer surface of the cornea is non-linear due to heat radiation. An iterative approach is used to treat the non-linear heat radiation term. The center corneal temperature is computed numerically and compared with values reported in the literature. It appears that the boundary element method calculates the normal heat flux more accurately than the finite element method on the corneal surface, especially near its edges.

* Author for correspondence (W. T. Ang)
E-mail: mwtang@ntu.edu.sg
http://www.ntu.edu.sg/home/mwtang/

Accepted for publication in
Engineering Analysis with Boundary Elements
(status as on 3 October 2006).
When the article is in press online, more details may be obtained by clicking:
http://doi.dx.org/10.1016/j.enganabound.2006.09.011

1 Introduction

In recent years, the boundary element method has become more popular as a numerical tool for analyzing heat transfer processes in biological systems. Chan [1] applied the method for the numerical solution of the Pennes bioheat equation and obtained numerical results that were in good agreement with analytical solutions. In [1], the fundamental solution in the form of a modified Bessel function was used to derive the appropriate boundary integral equation for the bioheat equation with the blood perfusion term. An alternative approach for analyzing the same bioheat equation, as given in Lu et al. [2], made use of the simpler fundamental solution for the Laplace equation. The resulting formulation would contain a domain integral which may be reduced approximately to a boundary integral by the dual reciprocity method. Poljak et al. [3] presented a boundary element analysis of heat transfer in the human body exposed to electromagnetic waves.

In the present paper, the boundary element method is applied to analyze the steady state temperature distribution in a two-dimensional model of the human eye. The earliest reported model for heat transfer in the eye was for a rabbit eye subject to electromagnetic waves (Emery et al. [4] and Guy et al. [5]). It was solved by the finite element method and the numerical results were reported to be in good agreement with data from experimental measurements. Scott [6] and Amara [7] used the finite element method to determine the steady state temperature in two-dimensional models of the human eye. In some earlier studies involving relatively simpler ocular models, the finite difference method was used to solve the governing equations numerically (see, for example, Lagendijk [8] and Okuna [9]). More recently, Hirata et al. [10], [11] applied the finite difference time domain method to study the temperature rise in the human eye exposed to electromagnetic waves.

There are some good reasons for using the boundary element method in

the analysis of bioheat transfer in the human eye. Firstly, the method requires only the boundary of the solution domain to be discretized. It helps not only to reduce the requirement on computer memory, but is also particularly advantageous in analyzing human eye models which comprise several sub-regions with different material properties and rather complicated geometries. Secondly, unlike the finite element or finite difference methods that solve for not necessarily wanted values of the temperature inside the whole eye, the boundary element method solves for the only unknown temperature or heat flux on the boundaries. Temperature and heat flux inside the eye may then be calculated as a post processing procedure, if needed. Current technology for eye temperature measurement uses infra-red thermography in which the temperature profile on the corneal surface is captured and displayed on a color- coded monitor. The corneal surface forms part of the boundary for the human eye. Knowing the temperature on the corneal surface is often sufficient for comparison with infra-red thermograms. Thirdly, the boundary element method is in general more accurate than the finite element method in computing secondary variables such as the heat flux.

2 A mathematical model of the human eye

As in Ng and Ooi [12], a two-dimensional model of the human eye as sketched in Figure 1 is considered here. In reality, in between the sclera and the vitreous, one may find two tissue layers known as the retina and the choroid. For simplicity, since these layers are relatively thin, they are modeled together with the sclera and the optic nerve as a single homogeneous region.

The thermal conductivities of the sclera, vitreous, lens, aqueous humor, iris and cornea may be found in the literature. They are given in Table 1. Each of the subdomains is assumed to be thermally isotropic and homogeneous.

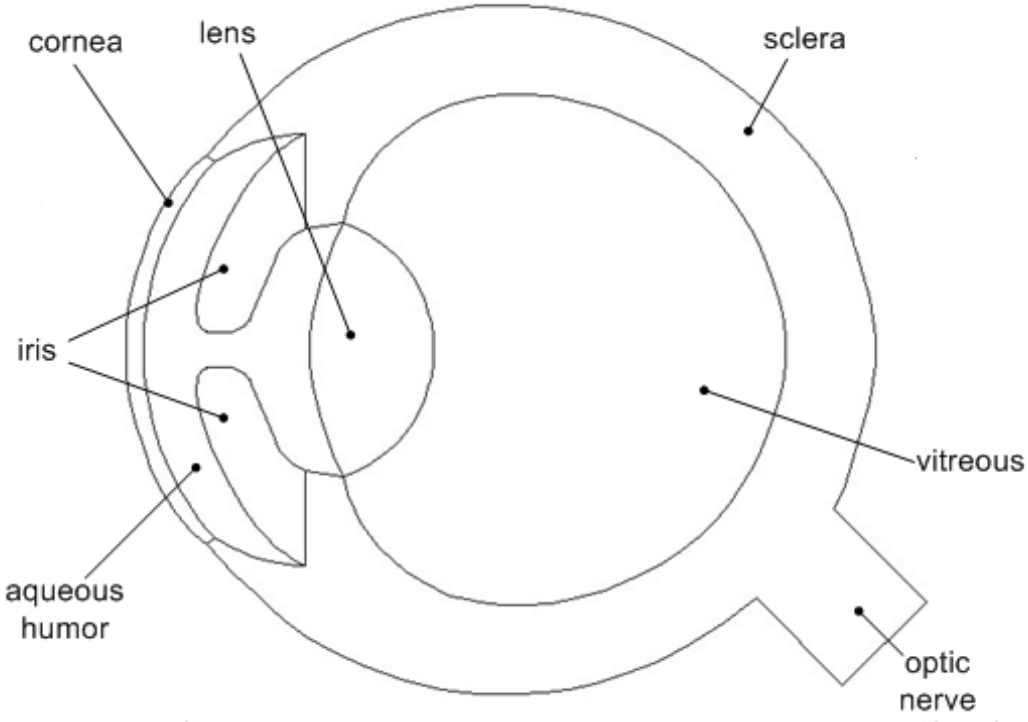

Figure 1. A sketch of the model.

Table 1. Thermal conductivities of the subdomains in the human eye.

Subdomain	**Thermal conductivity** (in $\mathrm{Wm}^{-1}(^{\circ}\mathrm{C})^{-1}$)	**Reference**
Cornea	0.58	Emery et al. [4]
Aqueous humor	0.58	Emery et al. [4]
Iris	1.0042	Cicekli [13]
Sclera	1.0042	Cicekli [13]
Lens	0.40	Lagendijk [8]
Vitreous	0.603	Scott [6]

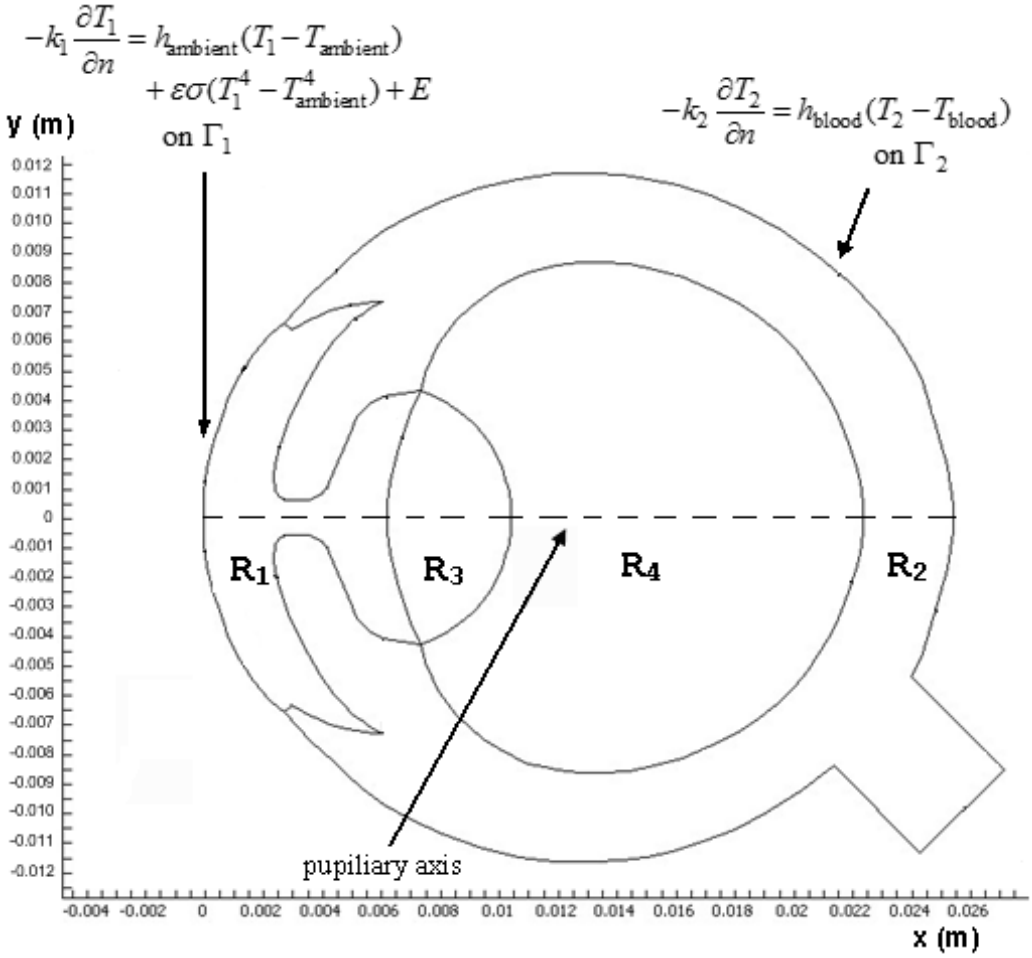

Figure 2. The four homogeneous regions and exterior boundary conditions.

The temperature distribution in the eye is assumed to be in steady-state condition. If the blood perfusion and the metabolic heat generation terms in the Pennes bioheat equation are neglected, the equation of flow of heat inside the eye may be reduced to the two-dimensional Laplace equation. Under such assumptions, since the cornea and the aqueous humor are contiguous and their thermal conductivities are of the same value, they are modeled as

a single homogeneous region denoted by R_1 in Figure 2. Similarly, the iris and the sclera are taken to be the homogeneous region R_2. The lens and the vitreous occupy the homogeneous regions R_3 and R_4 respectively. The exterior boundary of the eye comprises the cornea surface Γ_1 and the outer part Γ_2 of the sclera. Note that the measurement unit for the length along the x and y axes in Figure 2 is meter.

If the steady-state temperature in R_i is denoted by T_i then the heat flow is governed by

$$\nabla^2 T_i = 0 \text{ in } R_i \ \ (i = 1, 2, 3, 4), \tag{1}$$

where ∇^2 denotes the Laplacian operator.

The cornea is the only region in the eye that is exposed to the environment. At an ambient temperature lower than the corneal surface temperature, heat is extracted away from the eye via convection and radiation. A layer of tear film sits on top of the cornea. This layer is constantly evaporated and refreshed through the blinking of the eyelids. Besides convection and radiation, the evaporation of tears increases the cooling rate on the corneal surface. The loss of heat from the cornea generates a flow of heat flux from the regions of high temperature inside the eye to the corneal surface. Thus, the boundary condition on the corneal surface Γ_1 (the exterior boundary of the region R_1 in Figure 2) may be written as (see, for example, Scott [6])

$$-k_1 \frac{\partial T_1}{\partial n} = h_{\text{ambient}}(T_1 - T_{\text{ambient}}) + \varepsilon\sigma(T_1^4 - T_{\text{ambient}}^4) + E \ \text{ on } \Gamma_1, \tag{2}$$

where k_1 is the thermal conductivity of the cornea, $\partial T_1/\partial n$ is the rate of change of the temperature T_1 in the direction of the outward unit vector to R_1, h_{ambient} is the heat transfer coefficient related to the convection process in the surrounding environment, T_{ambient} is the temperature of the surrounding environment, ε and σ are the corneal emissivity and the Stefan-Boltzmann

constant respectively, and E is the loss in heat flux due to evaporation of tears . Note that the non-linear term in (2) models the heat transfer process by radiation.

On the exterior boundary Γ_2 of the region R_2, heat enters the eye system through the flow of blood. This may be modeled by using the boundary condition

$$-k_2 \frac{\partial T_2}{\partial n} = h_{\text{blood}}(T_2 - T_{\text{blood}}) \text{ on } \Gamma_2, \tag{3}$$

where k_2 is the thermal conductivity of the sclera, $\partial T_2/\partial n$ is the rate of change of the temperature T_2 in the direction of the outward unit vector to R_2, h_{blood} is the heat transfer coefficient related to the convection process in the blood, and T_{blood} is the temperature of the blood.

The values of control parameters (such as ε, σ and h_{blood}) related to the boundary conditions in (2) and (3) may be chosen as in Ng and Ooi [12]. Refer to Table 2.

The interfaces between the different contiguous regions are given by

$$\begin{aligned}
T_1 &= T_2 \text{ and } k_1 \frac{\partial T_1}{\partial n} = k_2 \frac{\partial T_2}{\partial n} \text{ on } I_{12}, \\
T_1 &= T_3 \text{ and } k_1 \frac{\partial T_1}{\partial n} = k_3 \frac{\partial T_3}{\partial n} \text{ on } I_{13}, \\
T_2 &= T_4 \text{ and } k_2 \frac{\partial T_2}{\partial n} = k_4 \frac{\partial T_4}{\partial n} \text{ on } I_{24}, \\
T_3 &= T_4 \text{ and } k_3 \frac{\partial T_3}{\partial n} = k_4 \frac{\partial T_4}{\partial n} \text{ on } I_{34},
\end{aligned} \tag{4}$$

where k_i is the thermal conductivity of R_i, I_{ij} denotes the interface between R_i and R_j and $\partial T_i/\partial n$ (on the interface) denotes the rate of change of T_i in the direction of a normal vector to the interface.

The human eye model of interest here is mathematically defined by (1) together with (2), (3) and (4).

Table 2. Control parameters for the exterior boundary conditions.

Control parameter	**Value**
Blood temperature T_{blood} (°C)	37
Ambient temperature T_{ambient} (°C)	25
Emissivity of cornea ε	0.975
Blood convection coefficient h_{blood} ($\text{Wm}^{-2}(^{\circ}\text{C})^{-1}$)	65
Ambient convection coefficient h_{ambient} ($\text{Wm}^{-2}(^{\circ}\text{C})^{-1}$)	10
Heat flux loss due to tear evaporation E (Wm^{-2})	40
Stefan-Boltzmann constant σ ($\text{Wm}^{-2}(^{\circ}\text{C})^{-4}$)	5.67×10^{-8}

3 Boundary element approach

A boundary element approach for the numerical solution of (1) subject to (2), (3) and (4) is outlined here.

The governing equation (1) may be recast in the integral form (see, for example, Clements [14])

$$\begin{aligned} c(\xi,\eta)T_i(\xi,\eta) &= \int_{\partial R_i} (T_i(x,y)\frac{\partial}{\partial n}[G(x,y;\xi,\eta)] \\ &\quad -G(x,y;\xi,\eta)\frac{\partial}{\partial n}[T_i(x,y)])ds(x,y) \\ &\quad \text{for } (\xi,\eta) \in R_i \cup \partial R_i, \end{aligned} \tag{5}$$

where ∂R_i denotes the boundary of the region R_i, $c(\xi,\eta) = 1$ if (ξ,η) lies in the interior of R_i, $c(\xi,\eta) = 1/2$ if (ξ,η) lies on a smooth part of ∂R_i, $\partial f/\partial n$ denotes the rate of change of f in the direction of the outward unit vector to R_i, and $G(x,y;\xi,\eta)$ is the fundamental solution of the two-dimensional Laplace equation as given by

$$G(x,y,\xi,\eta) = \frac{1}{4\pi}\ln([x-\xi]^2 + [y-\eta]^2). \tag{6}$$

Note that the interfaces between two contiguous regions in the human eye model may be parts of the boundary ∂R_i. For example, ∂R_1 consists of Γ_1 and the interfaces I_{12} and I_{13}.

Now if T_i and $\partial T_i/\partial n$ (which is essentially the heat flux) are known at all points on ∂R_i then then the temperature at any point (ξ, η) in R_i may be computed by evaluating approximately the boundary integral in (5). The heat flux components at any interior point (ξ, η) may also be computed directly by differentiating (5) partially with respect to ξ and η. Now if the non-linear radiation term in the boundary condition on the corneal surface is ignored (as done in some studies), the integral equation (5) together with (2), (3) and (4) may be discretized to set up a system of linear algebraic equations for finding approximately the values of T_i and $\partial T_i/\partial n$ over boundary elements on the exterior boundary $\Gamma_1 \cup \Gamma_2$ and the interfaces between the different regions of the eye. For details of such a procedure, one may refer to, for example, Clements [14] and Brebbia et al. [15]. The coefficients of the linear algebraic equations may be evaluated either numerically or analytically. If discontinuous linear elements are used, analytical formulae for the coefficients may be found in Ang [16]. The analytical formulae for constant elements may also be recovered as a special case from the results in [16].

The presence of the non-linear term in (2) slightly complicates matter, but may be easily be dealt with by using an iterative procedure as follows.

The temperature T_i is obtained through consecutive approximations $T_i^{(0)}$, $T_i^{(1)}, T_i^{(2)}, \cdots$. Assuming that $T_1^{(m-1)}$ is known, one uses the standard boundary element procedure to discretize (5) together with (3), (4) and (in the place of the non-linear condition (2)) the approximate linear boundary condition given by

$$-k_1 \frac{\partial T_1}{\partial n} = h_{\text{ambient}}(T_1 - T_{\text{ambient}}) + \varepsilon\sigma([T_1^{(m-1)}]^4 - T_{\text{ambient}}^4) + E \quad \text{on } \Gamma_1, \tag{7}$$

in order to set up a system of linear algebraic equations for determining $T_i^{(m)}$ and $\partial T_i^{(m)}/\partial n$ on the boundary $\Gamma_1 \cup \Gamma_2$ and the interfaces. Thus, one may begin with the initial approximation $T_1^{(0)} = T_{\text{ambient}}$ on Γ_1 in order to solve

for $T_i^{(1)}$ and $\partial T_i^{(1)}/\partial n$ on the boundary $\Gamma_1 \cup \Gamma_2$ and all the interfaces. The procedure may be repeated to obtain higher and higher order approximations for T until the criterion

$$|T_1^{(m)} - T_1^{(m-1)}| < \epsilon \quad \text{on } \Gamma_1, \tag{8}$$

where ϵ is a pre-selected real number of sufficiently small magnitude, is satisfied.

For the purpose here, ϵ is taken to be 1×10^{-5}. In the numerical results presented below, not more than 8 iterations are needed to achieve the convergence defined by the criterion (8).

4 Numerical results

With the model in Section 2 and the data in Tables 1 and 2, the boundary element approach outlined in Section 3 is used to compute the temperature distribution in the human eye. The exterior boundary $\Gamma_1 \cup \Gamma_2$ of the eye and the interfaces I_{12}, I_{13}, I_{24} and I_{34} between the different ocular regions are discretized into many short straight line elements. The temperature and the heat flux are approximated as constants (to be determined) over each boundary element, that is, constant elements are used. To carry out the calculation, 470 boundary elements are used, with 76 of them on the corneal surface Γ_1.

It is obvious from Figure 2 that a point lying on the corneal surface Γ_1 may be uniquely determined by its y coordinate. Figure 3 gives a plot of the temperature on the corneal surface Γ_1 (as obtained from the boundary element method) against the y coordinate of points on Γ_1. It appears that the temperature is minimum at the center of the corneal surface, that is, at the point $(0, 0)$.

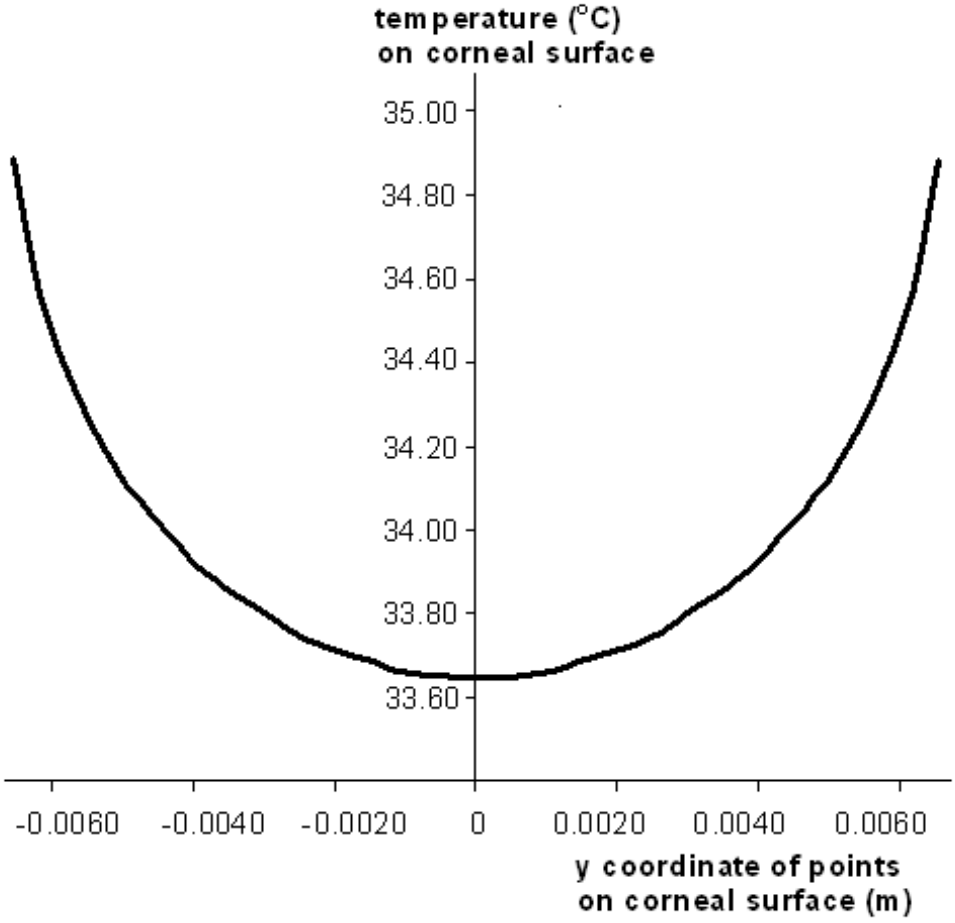

Figure 3. Temperature on corneal surface Γ_1.

Table 3. Values of the temperature at the center of the corneal surface.

Method	**Temperature** (°C)
Boundary element method (present work)	33.65
Finite element method (Ng and Ooi [12])	33.68
Finite element method (Scott [6])	33.25
Finite element method (Amara [7])	33.713
Experiment (Mapstone [17])	34.80
Experiment (Rysä and Sarvaranta [18])	34.50
Experiment (Fielder et al. [19])	33.40
Experiment (Efron et al. [20])	34.30
Experiment (Morgan et al. [21])	33.50
Experiment (Craig et al. [22])	33.82

The numerical value of the temperature at the center of the corneal surface is found to be 33.65°C. It is compared in Table 3 with values reported by other researchers. Ng and Ooi [12] used exactly the same mathematical model for the human eye as the one considered here, but solved it differently by using the finite element method provided by the commercialized software package COMSOL Multiphysics 3.2. Thus, it is perhaps not surprising that the numerical value obtained here agrees the most closely with the one reported in Ng and Ooi [12]. In [12], as many as 8557 domain elements were

employed in the finite element calculation. The human eye models in Scott [6] and Amara [7] differ from the one used here in details such as the values of the thermal conductivities used for the different regions of the eye and the modeling of heat loss through the corneal surface. A greater difference between the numerical values (of the temperature at the center of the corneal surface) in [6] and [7] and the one obtained here are only to be expected.

Experimental measurements of the temperature on the corneal surface may be obtained by using infra-red thermography. Some experimentally obtained values of the temperature at the center of the corneal surface are listed in Table 3. In Table 3, the numerical value of 33.65°C obtained here (using the boundary element method) is somewhere within the temperature range between the lowest and the highest experimentally obtained values (that is, between 33.4°C and 34.8°C).

Since the numerical values of the temperature at the center of Γ_1 as computed using the boundary element method here and the finite element method by Ng and Ooi [12] agree very closely, it may be of interest to compare the temperature obtained by the two methods at other points in the interior of the eye.

Figure 4 compares the temperature from the two methods along the horizontal pupiliary axis (the dotted horizontal line shown in Figure 2). As expected, the numerical values of the temperature along the pupliary axis obtained using the boundary element method are in good agreement with those from the finite element method. The temperature on the pupiliary axis is observed to increase from 33.65°C at the center of the corneal surface to a higher temperature of 36.5°C or thereabout at the sclera.

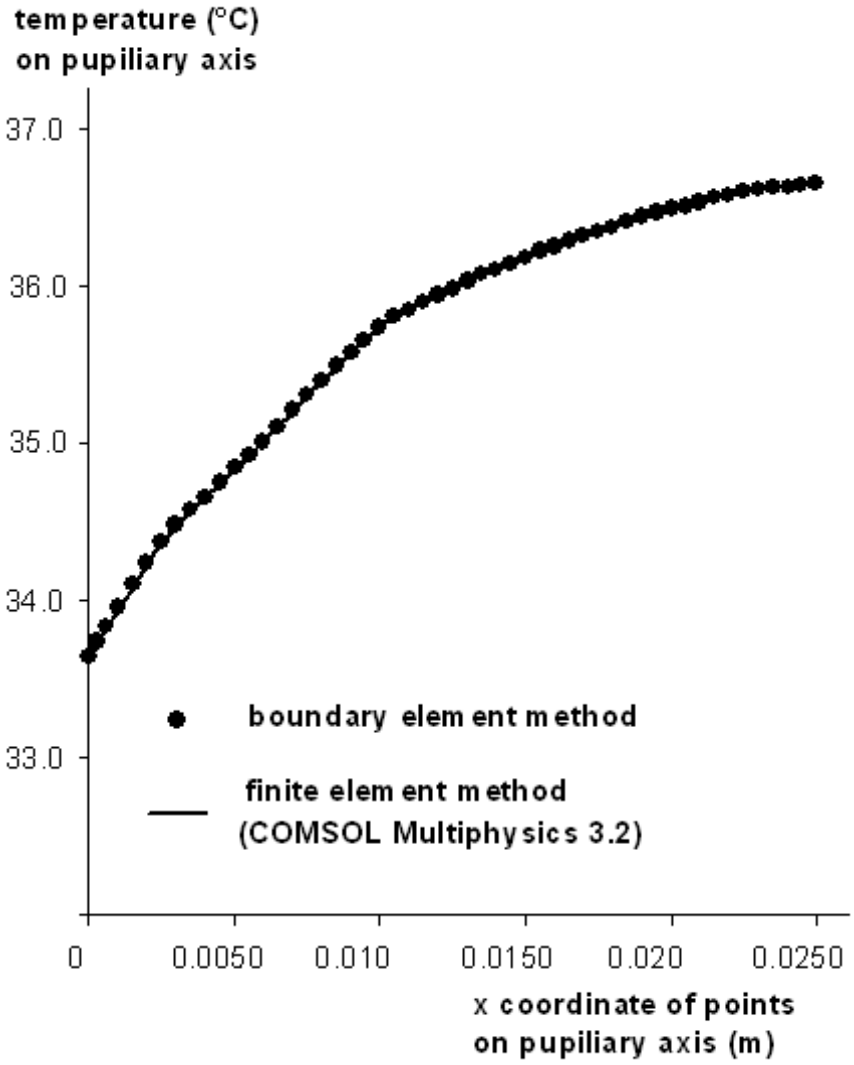

Figure 4. Temperature on the pupiliary axis.

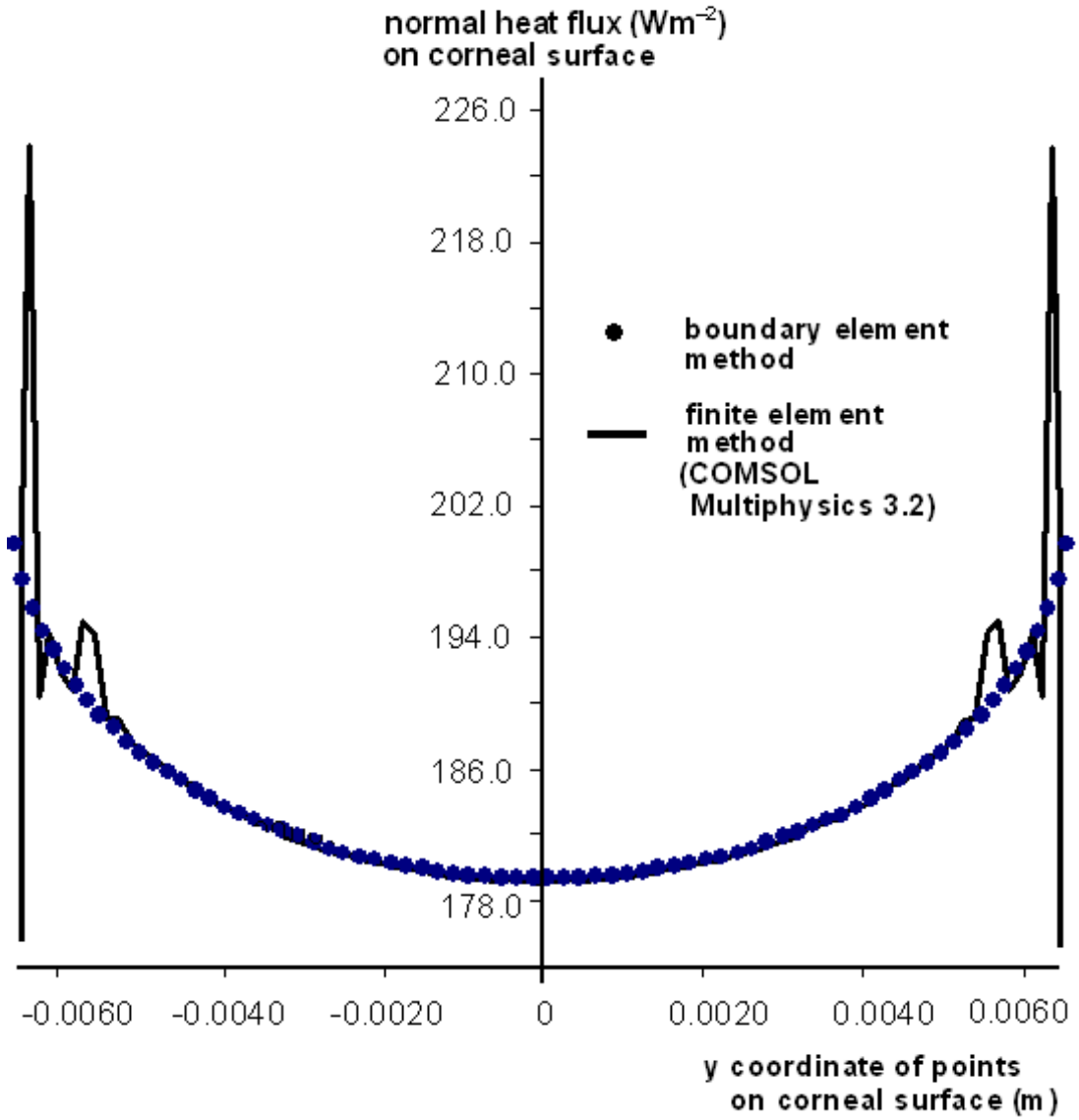

Figure 5. Normal heat flux on the corneal surface.

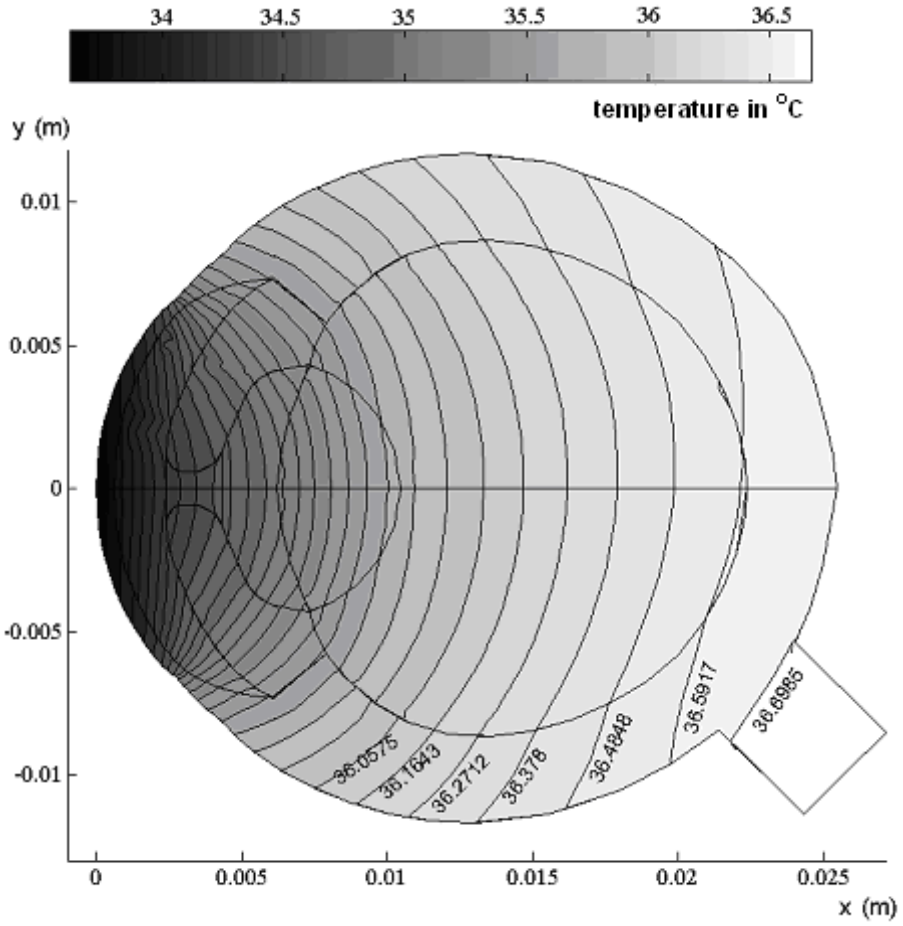

Figure 6. Temperature profile throughout the entire eye.

As the boundary element method is known to be in general more accurate than the finite element method in computing secondary variables such as the heat flux, a comparison of the two methods for computing the normal heat flux on the corneal surface is given in Figure 5. The finite element method in the commercialized software COMSOL Multiphysics 3.2 returns as an output the numerical values of the normal flux. It is clear from Figure 5 that there is a good agreement between the numerical values of the normal heat flux from

the finite element and the boundary element methods on the corneal surface, except at points near the edges of the corneal surface. Near the edges of the corneal surface, the finite element method gives numerical values which fluctuate wildly. The numerical values from the boundary element method do not behave erratically near the edges of the corneal surface. Instead, they appear to be varying smoothly across the surface. This seems to suggest that the boundary element method returns more reliable values of the normal heat flux than the finite element method near the edges of the corneal surface.

Figure 6 shows the temperature profile throughout the entire eye together with some isotherms as computed by the boundary element method. An isotherm farther to the right has a higher temperature. The temperature becomes closer to the blood temperature (37°C) at the posterior of the eye at the sclera . In fact, one may observe in Figure 6 that the temperature is very close to 37°C at where the optic nerve is. From a biological standpoint, such an observation is to be expected, as heat is transfered by blood to the eye through the exterior boundary of the sclera.

5 Summary and discussion

The boundary element method is applied to analyze the steady-state temperature in a two-dimensional model of the human eye. The cross section of the eye as depicted in Figures 1 and 2 is chosen as the solution domain of the two-dimensional model for at least two reasons. Firstly, it contains all the important tissue components (such as the lens and iris) of the human eye. Secondly, one may find the largest range of temperature across the chosen cross section. For example, along the pupiliary axis, the temperature ranges from the lowest at the center of the outer surface of the cornea (at about 34°C) to the highest at the outer surface of the sclera (near blood temperature of about 37°C). A basic assumption made in the two-dimensional model

is that the variation of the temperature is comparatively small along any direction that is perpendicular to the cross section of the eye shown in Figures 1 and 2. To investigate the validity of such an assumption, a three-dimensional model of the human eye (to be solved using the boundary element method) is currently being developed.

For the two-dimensional model here, the temperature distribution is computed by the boundary element method, using practically realistic values for the thermal conductivities of the various tissue components and for control parameters such as the tear evaporation rate. The numerical value of the temperature at the center of the corneal surface is obtained and found to fall within the range of the values given by other numerical and experimental data reported in the literature. In addition, the numerical values of the temperature along the pupiliary axis and the normal heat flux on the corneal surface are also compared with those obtained by the finite element method provided in the software COMSOL Multiphysics 3.2. The two sets of numerical results show good agreement, except that the finite element method appears to perform very poorly in the computation of the normal heat flux near the edges of the corneal surface. The boundary element method appears to give more reliable values for the normal heat flux near the edges of the corneal surface. It should provide an interesting and viable alternative (which is advantageous in some aspects) to other numerical techniques for studying bioheat transfer in the human eye.

References

[1] Chan LC. Boundary element methods for biological systems. In: Leondes CT (editor), Computational Methods in Biophysics, Biomaterials, Biotechnology and Medical Systems: Algorithm Development, Mathe-

matical Analysis and Diagnostics, Vol.. 3, Mathematical Analysis Methods, Kluwer Academic Publishers, pp. 295-319, 2003.

[2] Lu W-Q, Liu J, Zeng Y. Simulation of the thermal wave propagation in biological tissues by the dual reciprocity boundary element method. Engineering Analysis with Boundary Elements 1998; 22: 167-174.

[3] Poljak D, Peratta A, Brebbia CA. The boundary-element electromagnetic-thermal analysis of human exposure to base station antennas radiation. Engineering Analysis with Boundary Elements 2004; 28 : 763-770.

[4] Emery AF, Kramar PO, Guy AW, Lin JC. Microwave induced temperature rises in rabbit eyes in cataract research. Journal of Heat Transfer 1975; 97: 123-128.

[5] Guy AW, Lin JC, Kramar PO, Emery AF. Effect of 2450-MHz radiation on the rabbit eye. IEEE Transactions on Microwave Theory Techniques 1975; MTT-23: 492-498.

[6] Scott JA. A finite element model of heat transport in the human eye. Physics in Medicine and Biology 1988; 33: 227-241.

[7] Amara EH. Numerical investigations on thermal effects of laser ocular media interaction. International Journal of Heat and Mass Transfer 1995; 38: 2479-2488.

[8] Lagendijk JJW. A mathematical model to calculate temperature distributions in human and rabbit eyes during hyperthermic treatment. Physics in Medicine and Biology 1982; 27: 1301-1311.

[9] Okuno T. Thermal effect of infra-red radiation on the eye: a study based on a model. Annals of Occupational Hygiene 1991; 35: 1-12.

[10] Hirata A, Matsuyama S. and Shiozawa T. Temperature rises in the human eye exposure to EM waves in the frequency range 0.6-6GHz. IEEE Transactions on Electromagnetic Compatibility 2000; 42: 386-393.

[11] Hirata A. Temperature increase in human eyes due to near-field and far field exposures at 900MHz, 1.5GHz and 1.9GHz. IEEE Transactions on Electromagnetic Compatibility 2005; 47 (1): 68-76.

[12] Ng EYK, Ooi EH. FEM simulation of the eye structure with bioheat analysis. Computer Methods and Programs in Biomedicine 2006; 82: 268-276.

[13] Cicekli U. Computational Model for Heat Transfer in the Human Eye using the Finite Element Method. M.Sc Thesis, Department of Civil and Environmental Engineering, Louisiana State University, 2003.

[14] Clements DL. Boundary Value Problems Governed by Second Order Elliptic Systems. London: Pitman; 1981.

[15] Brebbia CA, Telles JCF, Wrobel LC. Boundary Element Techniques: Theory and Applications in Engineering. Berlin/Heidelberg: Springer-Verlag; 1984.

[16] Ang WT. A time-stepping dual-reciprocity boundary element method for anisotropic heat diffusion subject to specification of energy. Applied Mathematics and Computation 2005; 162: 661-678.

[17] Mapstone R. Measurement of corneal temperature. Experimental Eye Research 1968; 7: 237-243.

[18] Rysä P, Sarvaranta J. Thermography of the eye during cold stress. Acta Ophthalmologica 1973; 123: 234-239.

[19] Fielder AR, Winder AF, Sheridaidah GAK, Cooke ED. Problems with corneal arcus. Transactions of the Ophtalmological Societies of the United Kingdom 1981; 101 (1): 22-26.

[20] Efron N, Young G, Brennan N. Ocular surface temperature. Current. Eye Research 1989; 8 (9): 901-906.

[21] Morgan PB, Soh MP, Efron N, Tullo AB. Potential applications of ocular thermography. Optometry and Vision Science 1993; 70 (7): 568-576.

[22] Craig JP, Singh I, Tomlinson A, Morgan PB, Efron N. The role of tear physiology in ocular surface temperature. Eye 2000; 14: 635- 641.